ISSN 1063-7761, Journal of Experimental and Theoretical Physics, 2018, Vol. 126, No. 3, pp. 430–439. © Pleiades Publishing, Inc., 2018.
Original Russian Text © A.V. Filippov, A.N. Starostin, V.K. Gryaznov, 2018, published in Zhurnal Eksperimental'noi i Teoreticheskoi Fiziki, 2018, Vol. 153, No. 3, pp. 514–524.

STATISTICAL, NONLINEAR, AND SOFT MATTER PHYSICS

Coulomb Logarithm in Nonideal and Degenerate Plasmas

A. V. Filippov[a,*], A. N. Starostin[a,b], and V. K. Gryaznov[c,d]

[a] *State Research Center of the Russian Federation Troitsk Institute for Innovation and Fusion Research, Troitsk, Moscow, 108840 Russia*

[b] *Moscow Institute of Physics and Technology (State University), Dolgoprudnyi, Moscow oblast, 141701 Russia*

[c] *Institute of Problems of Chemical Physics, Russian Academy of Sciences, Chernogolovka, Moscow oblast, 142432 Russia*

[d] *Tomsk State University, Tomsk, 634050 Russia*

**e-mail: fav@triniti.ru*

Received October 13, 2017

Abstract—Various methods for determining the Coulomb logarithm in the kinetic theory of transport and various variants of the choice of the plasma screening constant, taking into account and disregarding the contribution of the ion component and the boundary value of the electron wavevector are considered. The correlation of ions is taken into account using the Ornstein–Zernike integral equation in the hypernetted-chain approximation. It is found that the effect of ion correlation in a nondegenerate plasma is weak, while in a degenerate plasma, this effect must be taken into account when screening is determined by the electron component alone. The calculated values of the electrical conductivity of a hydrogen plasma are compared with the values determined experimentally in the megabar pressure range. It is shown that the values of the Coulomb logarithm can indeed be smaller than unity. Special experiments are proposed for a more exact determination of the Coulomb logarithm in a magnetic field for extremely high pressures, for which electron scattering by ions prevails.

DOI: 10.1134/S1063776118020115

1. INTRODUCTION

In the physics of plasma and astrophysics, the long-range nature of the Coulomb or gravitational interaction leads to the emergence of various diverging integrals. For example, this leads to divergence of the transport cross sections of collisions of electrons and ions with charged particles, and this divergence is observed for small as well as large values of the impact parameter. In analyzing the kinetic equation for electrons in the case when the Coulomb interaction prevails, Landau [1] introduced constraints on the impact parameter for eliminating divergences, which led to the emergence the Coulomb logarithm in the transport cross section of scattering of electrons by ions:

$$\Lambda = \ln\left(\frac{R_D}{r_0}\right). \tag{1}$$

Here, R_D is the highest value of the impact parameter, which was assumed in [1] to be equal to the Debye screening radius:

$$R_D = k_D^{-1}, \quad k_D^2 = k_{De}^2 + k_{Di}^2,$$
$$k_{De}^2 = \frac{4\pi e^2 n_e}{T_e}, \quad k_{Di}^2 = \frac{4\pi z_i^2 e^2 n_i}{T_i}, \tag{2}$$

where r_0 is the smallest impact parameter corresponding to scattering of an electron (ion) with a thermal energy through 90° (in the plasma physics, this quantity is usually referred to as the Landau radius), which, in the case of scattering of an electron by an ion, is defined as

$$r_0 = \frac{e^2 z_i}{T_e}, \tag{3}$$

e is the elementary charge; z_i is the ion charge number; T_e and T_i are the temperatures of electrons and ions in energy units, respectively; and n_e and n_i are the concentrations of electrons and ions, respectively.

Spitzer [2] introduced a quantity close to the Coulomb logarithm, which is equal to the ratio of right angle ($\pi/2$) to the scattering angle for an impact parameter equal to the mean distance between scattered particles interacting in accordance with the law of universal gravitation. In subsequent publications [3, 4], Spitzer with coauthors used the Landau definition for the Coulomb logarithm with the full Debye radius of the plasma, while in monograph [5], he proposed that only the electron Debye radius be used for determining the external cutoff radius.

Temko [6] derived the Fokker–Planck equation for a plasma proceeding from the chain of the Bogoliubov equations. In this approach, screening was taken into account in a natural way, and the Landau radius was used for a cutoff for small impact parameters. The fol-

lowing expression was obtained in [6] for the Coulomb logarithm:

$$\Lambda = \frac{1}{2}\ln\left(1 + \frac{R_D^2}{r_0^2}\right); \quad (4)$$

in contract to expression (1), it gives no negative values for the Coulomb logarithm.

Later, the Coulomb logarithm was studied in many publications (see, for example, [7–17] and the literature cited therein), and the theory of scattering in an ideal plasma was developed to such an extent that made it possible to refine the value of the numerical factor (which is different for different transport processes) in the argument in the Coulomb logarithm (see, for example, [7]). Spitzer believed that the accuracy of the scattering theory with the Coulomb logarithm is sufficient only for $\Lambda \gtrsim 10$, while in [9, 10] (see also [11]), it was proved that the accuracy is sufficient down to $\Lambda \approx 2$. Subsequently, the values of $\Lambda < 1$ were also considered in the literature [11–16]. In [15], the equalization of the temperatures of electrons and ions in a dense plasma was analyzed on the basis of the quantum-mechanical method of T matrices. Since this method is quite cumbersome, it was proposed that scattering cross sections based on the Landau–Spitzer approach be used with the Coulomb logarithm

$$\Lambda = \frac{1}{2}\ln\left(1 + \frac{b_{\max}^2}{r_0^2 + \lambda\!\!\!^{-2}_e/8\pi}\right). \quad (5)$$

Here, $b_{\max}$ is the maximal impact parameter defined by the relation

$$b_{\max} = R_{De}\exp\left(\frac{a_1 + a_2\ln\Lambda_0}{1 + \Lambda_0^{a_3}}\right),$$

parameters a_1, a_2, and a_3 are determined by the condition of the best approximation of the results of calculations based on the T-matrix method, and the following values of these parameters were obtained in [15]: $a_1 = 1.65$, $a_2 = 0.40$, $a_3 = 0.64$; $R_{De} = k_{De}^{-1}$ is the Debye radius for an electron, Λ_0 is the Coulomb logarithm defined as

$$\Lambda_0 = \frac{1}{2}\ln\left(1 + \frac{R_{De}^2}{r_0^2 + \lambda\!\!\!^{-2}_e/8\pi}\right), \quad (6)$$

$\lambda\!\!\!^{-}_e$ is the de Broglie wavelength for electrons,

$$\lambda\!\!\!^{-}_e = \sqrt{\frac{2\pi\hbar^2}{m_e T}}, \quad (7)$$

and m_e is the electron mass. It was noted in [15] that for a nondegenerate plasma with $n_e\lambda\!\!\!^{-3}_e < 0.1$ (n_e is the electron concentration), expression (5) gives the energy loss rate with an error of 15% for $\Lambda_0 > 2 \times 10^{-2}$, while, for $\Lambda_0 > 5 \times 10^{-3}$, the error does not exceed 30%. For higher values of Λ_0, the accuracy was considerably higher. It should be noted that for determining the de Broglie wavelength in a degenerate plasma, it was proposed in [9] (as well as in our work [18]) that the Fermi energy be used instead of the electron temperature. Expression (5) gives the values of the Coulomb logarithm close to and slightly smaller than unity (i.e., it "corrects" small values of $\Lambda_0 \ll 1$ in the region of weak nonideality of the plasma).

In [18], in determining the electrical conductivity of a dense hydrogen plasma, we also used the approach based on the Coulomb logarithm; its values in the region of strong ionization of the plasma turned out to be much smaller than unity, which casts a shade of doubt concerning the applicability of the approach used for describing the electron transport in this range of parameters. For this reason, the present study is devoted to a more detailed analysis of this problem. It should be noted that the approximate approach based on the Coulomb logarithm was chosen because exact calculations of the scattering cross section require very long time (as in the above remark concerning the T-matrix method).

At high pressures, the so-called pressure ionization occurs [19], and any substance becomes in the general case a nonideal and degenerate plasma. The determination of the transport properties of electrons in a nonideal plasma remains one of unsolved problems in the kinetic theory. For solving this problem, approximate methods are used, including one of the most widely used approaches based on the Born approximation with subsequent correction of results by introducing the Coulomb logarithm. It should be noted that scattering in a nonideal plasma is a multiparticle process, and the accuracy of modern experiments does not permit the determination of even exact order of magnitude of the Coulomb logarithm. Therefore, meticulous analysis of theoretical methods for determining the Coulomb logarithm is of considerable interest.

2. TRANSPORT CROSS SECTION OF ELECTRON SCATTERING BY IONS

Ziman [20–24] introduced and actively used the concept of an "atom" (ion with a screening electron cloud) for describing the transport properties of electrons in metals. Scattering of an electron from such an atom occurs with a pseudopotential equal to the screened Debye potential, and the interaction of atoms with one another is described by the same potential. It was assumed in [20–24] that only electrons participate in screening; randomness or orderliness in the arrangement of such "atoms" (henceforth referred to just as ions) is taken into account by the static structure factor. This theory was quite successful in the description of transport properties of electrons in various metals and their alloys; for this reason, we will also use this approach in this study.

In the general case, screening by electrons in a plasma is described by the expression [25, 26]

$$k_{De}^2 = \frac{8\pi e^2}{T}\frac{1}{\lambda\!\!\!^{-3}_e}\mathcal{F}_{-1/2}(\eta_e), \quad (8)$$

where T is the electron temperature, $\eta_e = \mu_e/T$, μ_e being the chemical potential of the electron gas; $\mathcal{F}_{-1/2}(\eta_e)$ is the Fermi–Dirac integral, which is defined by the relation [27]

$$\mathcal{F}_k(\eta_e) = \frac{1}{\Gamma(k+1)}\int_0^\infty \frac{x^k dx}{\exp(x-\eta_e)+1}, \quad (9)$$

$\Gamma(x)$ being the gamma function. The electron concentration is given by

$$n_e = \frac{2}{\lambda\!\!\!^{-3}_e}\mathcal{F}_{1/2}(\eta_e). \quad (10)$$

Combining expressions (8) and (10), we obtain

$$k_{De}^2 = k_{De,0}^2\frac{\mathcal{F}_{-1/2}(\eta_e)}{\mathcal{F}_{1/2}(\eta_e)}, \quad (11)$$

where $k_{De,0}$ is the electron screening constant in the nondegenerate case:

$$k_{De,0}^2 = \frac{4\pi e^2 n_e}{T}. \quad (12)$$

It should be noted that at room temperature and $n_e \lesssim 10^{18}$ cm^{-3}, the electron screening constant almost coincides with expression (12) (see Fig. 1), while in the strongly degenerate case, we have

$$k_{De}^2 = \frac{m_e e^2}{\pi^2\hbar^2}\left(\frac{3n_e}{\pi}\right)^{1/3}. \quad (13)$$

In our calculations, we determined the value of reduced chemical potential η_e using expression (10) from the preset electron concentration n_e, and then screening constant k_{De} was found from formula (8) or (11). The Fermi–Dirac integrals were calculated in accordance with [27]. We can also write the expression for the mean kinetic energy of electrons:

$$\langle\varepsilon_e\rangle = \frac{3}{2}T\frac{\mathcal{F}_{3/2}(\eta_e)}{\mathcal{F}_{1/2}(\eta_e)}. \quad (14)$$

In a nondegenerate plasma, we have $\langle\varepsilon_e\rangle = (3/2)T$, while in a strongly degenerate plasma, $\langle\varepsilon_e\rangle = (3/5)\varepsilon_F$, where ε_F is the Fermi energy:

$$\varepsilon_F = (3\pi^2 n_e)^{2/3}\frac{\hbar^2}{2m_e}. \quad (15)$$

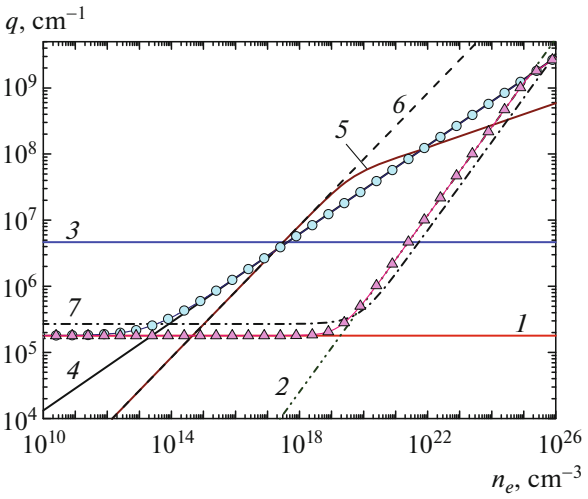

Fig. 1. Dependences of the basic parameters of the plasma, which have the dimension of the reciprocal length and determine the boundary value of wavevector q_m, on the electron concentration at $T = 300$ K, $z_i = 1$. Curve *1* is the reciprocal Landau radius (3); (*2*) reciprocal Landau radius with the Fermi energy instead of temperature; (*3–6*) $q_m = 2/\lambda\!\!\!^{-}_e$ (*3*), $2k_F$ (*4*), k_{De} (*5*), and k_{Di} (*6*); (*7*) reciprocal Landau radius with mean kinetic energy $\langle\varepsilon_e\rangle$, (△) $q_m = q_{mS}$ (27); (○) $q_m = q_{mZ}$ (28).

The transport cross section of electron scattering by ions taking into account the ion–ion correlation is defined as [28]

$$Q_{ei}(\varepsilon_e) = \frac{\pi z_i^2 e^4}{\varepsilon_e^2}\Lambda_{ei}, \quad (16)$$

where ε_e is the electron energy, Λ_{ei} is the Coulomb logarithm,

$$\Lambda_{ei} = \int_0^{q_m}\frac{k^3}{(k^2+k_s^2)^2}S_i(k)dk, \quad (17)$$

$S_i(k)$ is the static structure factor describing the correlation of ions with the interaction potential

$$U_{ii}(R) = \frac{z_i^2 e^2}{R}\exp(-k_s R), \quad (18)$$

R is the spacing between ions, k_s is the screening constant, and q_m is the maximal value of the wavevector (which is determined by the maximal value of the electron momentum transferred to an ion during the collision). It was assumed in [20] that $q_m = 2k_F$ (the maximal value of the transferred momentum for an electron on the Fermi surface is $2\hbar k_F = 2\sqrt{2m_e\varepsilon_F}$), where k_F is the wavelength of an electron on the Fermi surface:

$$k_F = (3\pi^2 n_e)^{1/3}. \quad (19)$$

It was assumed in [18] that

$$q_m = \min\{E_T/z_i e^2, 2/\lambda\!\!\!^{-}_e\}, \quad (20)$$

where E_T was assumed to be equal to temperature (in energy units) in the nondegenerate case and to the Fermi energy in the degenerate case; the de Broglie wavelength in these cases was also determined using the temperature or the Fermi energy.

In a rarefied plasma for which the ion–ion correlation can be disregarded, we have $S_i \approx 1$. In this case, we obtain from expression (17) (see [26, 29])

$$\Lambda_{ei} = \frac{1}{2}\left[\ln(1+\chi_i) - \frac{\chi_i}{1+\chi_i}\right], \quad (21)$$

where $\chi_i = (q_m/k_s)^2$. Using the static structure factor for ions in the Debye approximation ($z_i n_i = n_e$) [30],

$$S_{iD} = 1 - \frac{e^2 z_i^2}{T}\frac{4\pi n_i}{k^2 + k_s^2} \quad (22)$$

we obtain from expression (17) [18]

$$\Lambda_{ei} = \frac{1}{2}\left[\ln(1+\chi_i) - \frac{\chi_i}{1+\chi_i} - \frac{1}{2}\frac{z_i}{k_s^2}\frac{4\pi n_e e^2}{T}\frac{\chi_i^2}{(1+\chi_i)^2}\right]. \quad (23)$$

In this study, we determined the static structure factor for ions by solving numerically the Ornstein–Zernike (OZ) equation [31–33],

$$h(\mathbf{r}) = C(\mathbf{r}) + n_i\int h(\mathbf{r}_1)C(|\mathbf{r} - \mathbf{r}_1|)d\mathbf{r}_1, \quad (24)$$

where $g(r) = 1 + h(r)$ is the pair static structure function, $C(r)$ is the direct correlation function, and n_i is the ion concentration. For closing the OZ equation, we used the hypernetted-chain (HNC) approximation [34]:

$$C(\mathbf{r}) = \exp\left[-\frac{U_{ii}(\mathbf{r})}{T} + \gamma(\mathbf{r})\right] - \gamma(\mathbf{r}) - 1, \quad (25)$$

where $U_{ii}(r)$ is the interaction potential for the particles under investigation and $\gamma(r) = h(r) - C(r)$. In our case, we used Debye potential (18) for describing the ion–ion interaction. The hypernetted-chain approximation is found to be sufficiently accurate for describing Coulomb systems and systems of particles, the interaction of which is described by the Debye potential (see, for example, [35]).

The static structure factor is connected with the two-particle correlation function by the Fourier transform [32]:

$$S(k) = 1 + n_i\int [g(r) - 1]e^{-i\mathbf{k}\cdot\mathbf{r}}d\mathbf{r} = 1 + \frac{4\pi n_i}{k}\int_0^\infty h(r)\sin(kr)rdr. \quad (26)$$

The OZ equation was solved by iterations [36, 37]; for the initial solution, the values of the static structure factor in the Debye approximation (22) were specified. For accelerating the convergence, we used the procedure proposed in [38].

3. NUMERICAL CALCULATIONS AND DISCUSSION OF RESULTS

In this study, we consider two variants of determining the Debye screening constant taking into account ($k_s = k_D$) and disregarding ($k_s = k_{De}$) the contribution of the ion component. The value of boundary wavevector q_m was defined either in [18],

$$q_m = q_{mS} \equiv \min(r_0^{-1}\sqrt{1 + (\varepsilon_F/T)^2}, 2k_E), \quad (27)$$

or as the reciprocal Landau radius in a nondegenerate plasma with a transition to $2k_F$ in a degenerate plasma (as in [20]):

$$q_m = q_{mZ} \equiv \sqrt{r_0^{-2} + 4k_F^2}. \quad (28)$$

Here, k_E is the wavenumber determined from the mean electron kinetic energy (14):

$$k_E = \left(\frac{10}{3}\frac{\langle\varepsilon_e\rangle m_e}{\hbar^2}\right)^{1/2}. \quad (29)$$

which is transformed to the wavenumber of an electron with the Fermi energy in a strongly degenerate case. In this study, we performed calculations for four variants of the choice of the maximal value of the wavenumber and screening constant: (i) $k_s = k_{De}$, $q_m = q_{mZ}$; (ii) $k_s = k_D$, $q_m = q_{mZ}$; (iii) $k_s = k_{De}$, $q_m = q_{mS}$; and (iv) $k_s = k_D$, $q_m = q_{mS}$.

Analysis of various variants of the choice of the screening constant and the boundary value of the wavevector is dictated by the following circumstances. As noted above, the electron screening constant is used as the screening constant in a number of publications. Such a choice is justified in the case of metals, because ions are at the crystal lattice sites; however, in the case of a plasma with not very high values of the nonideality parameter (see Fig. 2, in which an increase of ordering in the ion distribution upon an increase in Γ is observed), the ion component also participates in the screening of the electric field of ions. The choice of the boundary value of the wavevector equal to $2k_F$ in the case of metal is obvious, because the transport is mainly executed by electrons with energies close to the Fermi surface; however, such a choice in the case of a plasma is questionable.

Figure 1 shows that the value of q_{mS}, which coincides with the reciprocal Landau radius for low electron concentrations, tends to the value equal to the reciprocal Landau radius determined when the Fermi energy is taken as temperature for an electron concentration on the order of 10^{19} cm^{-3}; as the concentration increases further to about 10^{25} cm^{-3}, the value of q_{mS}

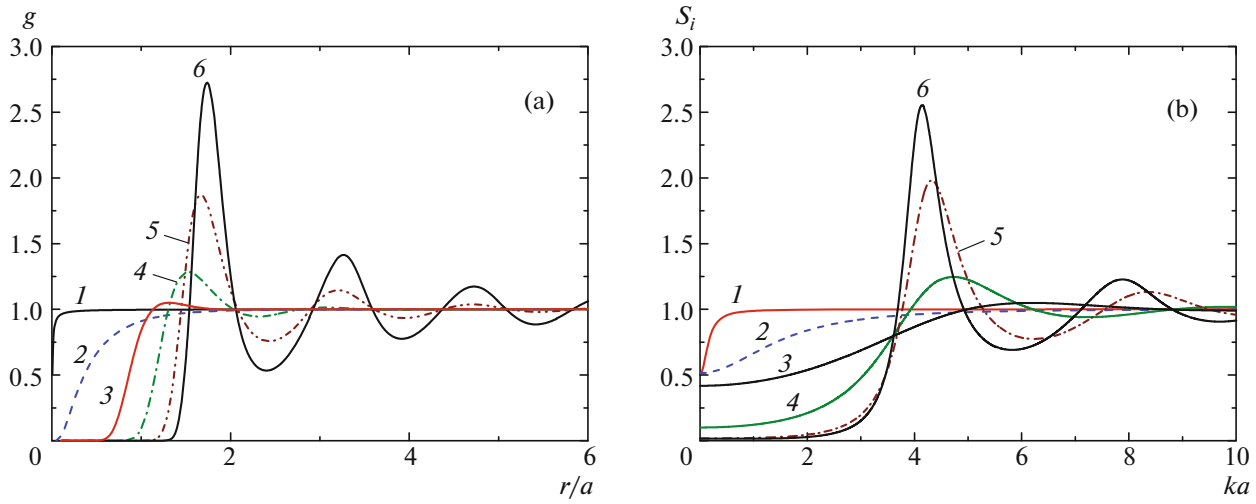

Fig. 2. (Color online) (a) Two-particle correlation function and (b) static structure factor for ions at $T = 300$ K, $z_i = 1$ for different values of the nonideality parameter $\Gamma = 4.2 \times 10^{-3}$ (*1*), 0.416 (*2*), 89.7 (*3*), 193 (*4*), 416 (*5*), and 897 (*6*).

tends to $2k_F$. It should be noted that the behavior of q_{mS} is very close to the behavior of the reciprocal Landau radius with mean kinetic energy $\langle\varepsilon_e\rangle$ instead of temperature (see curve *7* in Fig. 1). For low concentrations, the value of q_{mZ} coincides with r_0^{-1} and tends to $2k_F$ upon an increase in the concentration.

It can also be seen from Fig. 1 that the electron Debye radius for $n_e > 10^{18}$ cm^{-3} becomes sensitive to degeneracy at room temperature, and the electron screening constant becomes noticeably smaller than the ion screening constant.

Figure 2 shows the dependence of the two-particle correlation function and the static structure factor for ions with multiplicity of ionization $z_i = 1$ at $T = 300$ K on r/a and ka for different values of nonideality parameter Γ, which is defined as

$$\Gamma = \frac{e^2 z_i^2}{aT}, \quad a = \left(\frac{3}{4\pi n_i}\right)^{1/3}. \tag{30}$$

Using analogous dependences of the static structure factor, we calculated Coulomb logarithm (17). The inequality $k_{\max} > q_m$ usually held, but if it was violated, we set $S_i = 1$ in the range of $k_{\max} < k \le q_m$, were $k_{\max}$ is the maximal value of the wavevector in calculations of the static structure factor.

3.1. Calculations for $k_s = k_{De}$ and $q_m = q_{mZ}$ (Variant 1)

Figure 3 shows the dependences of the Coulomb logarithm on the electron concentration for variant 1. It can be seen that with increasing n_e, Λ_{ei} decreases and passes through a minimum at $n_e \sim 10^{19}$ cm^{-3}. Curve *2* calculated for $S_i = 1$ behaves analogously; therefore, we can conclude that the emergence of the minimum is not associated with variations of the static structure factor upon a change in the ion concentration. Comparing curves *1* and *2*, we can conclude that the inclusion of the ion–ion correlation contributes to the Coulomb logarithm even for $n_e \sim 10^{12}$ cm^{-3}, but this contribution becomes especially noticeable for $n_e > 10^{20}$ cm^{-3}, when correlations must be taken into account and lead to a substantial decrease in the electron scattering cross section.

It can be seen from Fig. 3 that the calculations with the static structure factor in the Debye approximation (22) are in good agreement with the calculations in which the static structure factor is determined from the OZ equation up to electron concentrations on the order of 10^{15} cm^{-3}; for higher concentrations, the discrepancy becomes noticeable. It should be noted that the approximation with $S_i \approx 1$ proves to be more exact in this range.

Figure 3 also shows the values of the Coulomb logarithm calculated using the classical formulas for a nondegenerate plasma (curve *4*). It can be seen that curve *4* for low n_e is close to the dependence $\ln(q_{mZ}/k_{De})$, which is the asymptotic form of the dependences (21) and (23) for $n_e \to 0$ (see [18]).

Figure 4 shows the corrections to the classical electron screening radius at different temperatures. It can be seen that at $T = 300$ K, the degeneracy effects for the electron component of the plasma become noticeable for $n_e \sim 10^{18}$ cm^{-3}; with increasing n_e, the screening properties of the electron gas become noticeably weaker. With increasing electron temperature, the screening effects are reduced, and the deviation of the correction from unity are observed for large values of n_e. For this reason, the minima of the Coulomb logarithm are also shifted towards higher electron concen-

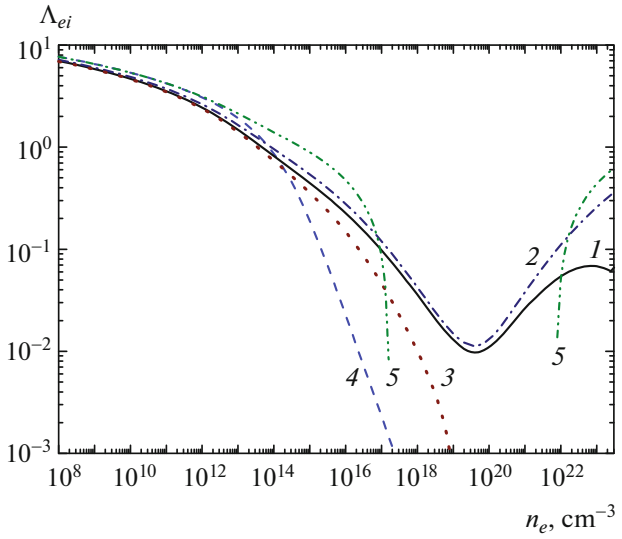

Fig. 3. Coulomb logarithm as a function of the electron concentration at $T = 300$ K, $z_i = 1$ with the boundary value of the wavevector $q_m = q_{mZ}$ disregarding the contribution of ions to screening, $k_s = k_{De}$. Curve *1* corresponds to numerical integration of relation (17), (*2*) (21), (*3*) (23), (*4*) (4) for the classical case, (*5*) $\Lambda_{ei} = \ln(q_{mZ}/k_{De})$.

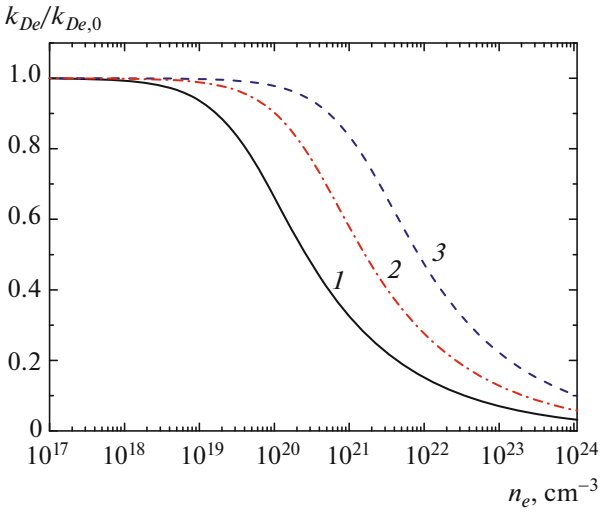

Fig. 4. (Color online) Degeneracy correction to the classical electron inverse screening radius at different temperatures: 300 (*1*), 1000 (*2*), and 3000 K (*3*).

trations upon an increase in temperature, which can clearly be seen in Fig. 5.

It can be seen from Fig. 5 that the values of the Coulomb logarithm in a nondegenerate plasma increase with temperature, which is associated with a decrease in the Landau radius, as well as with an increase in the screening radius. It can also be seen that formula (23) is a good approximation only for $n_e \sim 10^{15}$–10^{17} cm^{-3}, and ion–ion correlations in the region behind the minimum of Λ_{ei} must be taken into account more exactly than in the Debye approximation.

Comparison of the positions of minima of Λ_{ei} in Fig. 5 and of ratio k_F/k_{De} in Fig. 6 shows that these positions almost coincide. The emergence of a minimum of ratio k_F/k_{De} is associated with the following circumstance. Screening constant k_{De} on the left branch in the range of a nondegenerate plasma increases in proportion to $n_e^{1/2}$, while k_F increases as $n_e^{1/3}$; for this reason, their ratio decreases as $n_e^{-1/6}$. On the right branch behind the minimum, screening constant k_{De} in the range of the degenerate plasma increases as $n_e^{1/6}$ in accordance with relation (13); therefore, ratio k_F/k_{De} increases in proportion to $n_e^{1/6}$. This explains the emergence of the minimum of ratio k_F/k_{De} in the region of transition from the nondegenerate to degenerate plasma. This leads to the conclusion that the emergence of the minimum of the Coulomb logarithm is a consequence of suppression of screening of ions due to the degeneracy of the electron gas.

With increasing charge number of ions, the values of the Coulomb logarithm decrease (see Fig. 7) due to an increase in the Landau radius for small $n_e < 10^{14}$–10^{15} cm^{-3} (the theoretical curves with $S_i = 1$ for different values of z_i subsequently merge into one curve), while the differences for large n_e are due to differences in the static structure factors in Debye approximation (22), as well in those obtained from the OZ equation in the HNC approximation. As can be seen from

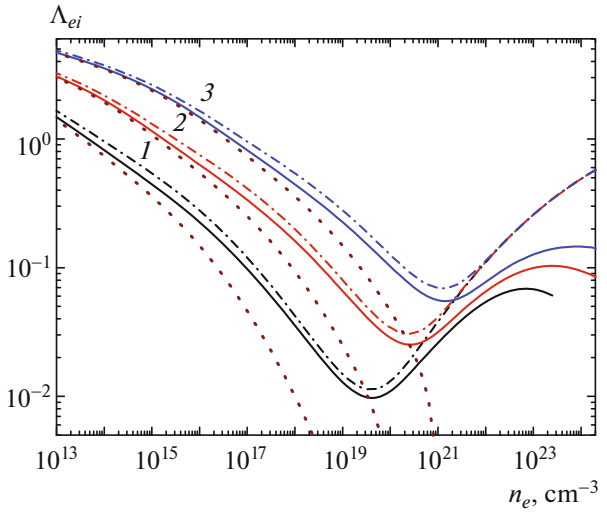

Fig. 5. (Color online) Coulomb logarithm as a function of the electron concentration for $z_i = 1$ with the boundary value of the wavevector $q_m = q_{mZ}$ disregarding the contribution of ions to screening, $k_s = k_{De}$ at different temperatures: 300 K (*1*); 1000 K (*2*), and 3000 K (*3*). Solid curves correspond to numerical integration of expression (17) with the static structure factor from the OZ equation in the HNC approximation; dot-and-dash curves correspond to formula (21) and dotted curves, to (23).

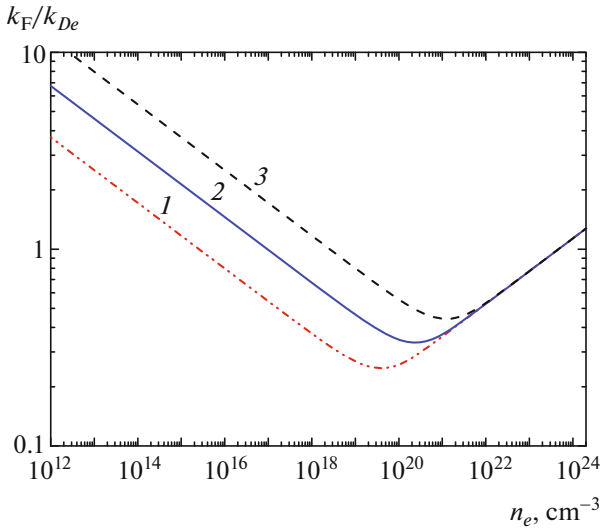

Fig. 6. (Color online) Dependences of the ratio of the Fermi wavenumber to the electron screening constant on the electron concentration at different temperatures: 300 (*1*), 1000 (*2*), and 3000 K (*3*).

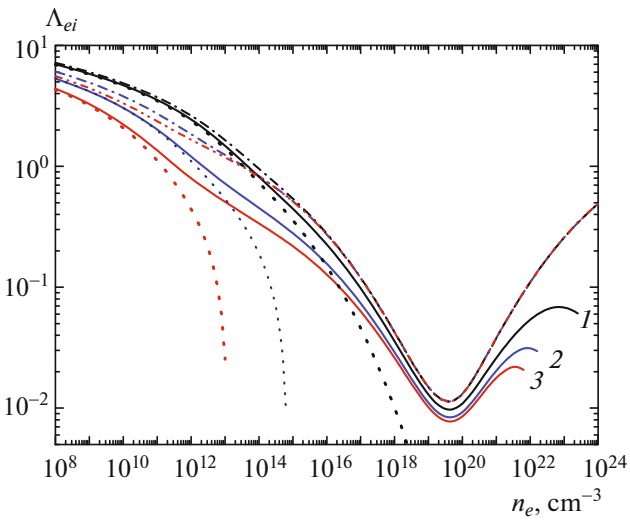

Fig. 7. (Color online) Coulomb logarithm as a function of the electron concentration at $T = 300$ K with the boundary value of the wavevector $q_m = q_{mZ}$ disregarding the contribution of ions to screening, $k_s = k_{De}$ at different values of the ion charge number $z_i = 1$ (*1*), 3 (*2*), and 5 (*3*). Solid curves correspond to numerical integration of expression (17) with the static structure factor from the OZ equation in the HNC approximation; dot-and-dash curves correspond to formula (21) and dotted curves, to (23).

Fig. 7, the Λ_{ei} minima are observed for the same value of n_e because the position of the k_F/k_{De} minimum is independent of z_i.

3.2. Calculations for $k_s = k_D$ and $q_m = q_{mZ}$ (Variant 2)

Figure 8 shows the dependences of the Coulomb logarithm in variant 2 ($k_s = k_D$ and $q_m = q_{mZ}$). It can be seen that the minimum disappears in this case, and only the singularity in the form of two slight inflections is left in the region of the minimum in variant 1. In this case, the calculations with the static structure factor in the Debye approximation turn out to be quite close to curve *1* up to $n_e \sim 10^{18}$ cm^{-3}, and the results of calculations with $S_i = 1$ almost coincide with the calculations in which S_i is obtained from the OZ equation. Therefore, we can conclude that the effect of the ion–ion correlation in this variant of calculations is negligibly weak. An analogous behavior is also observed at other temperatures (Fig. 9).

3.3. Calculations for $k_s = k_{De}$ and $q_m = q_{mS}$ (Variant 3) and $k_s = k_D$ and $q_m = q_{mS}$ (Variant 4)

In Fig. 10, the above four variants of calculation are compared. It can be seen that in calculations with $q_m = q_{mS}$, the values of the Coulomb logarithm are noticeably smaller than in calculations with $q_m = q_{mZ}$. The values of Λ_{ei} are found to be smaller in calculations with $k_s = k_D$ than with $k_s = k_{De}$. As can be seen from Fig. 10, the inclusion of the ion–ion correlation is important only in calculations disregarding screening by ions. An analogous pattern was also observed in calculations with $T = 300$, 1500, and 3000 K.

4. ELECTRICAL CONDUCTIVITY OF A NONIDEAL PLASMA

Apart from the Coulomb logarithm, we calculated the electrical conductivity of a plasma for the four variants of determining the Coulomb logarithm. The conductivity was determined using the Lorenz–Bloch

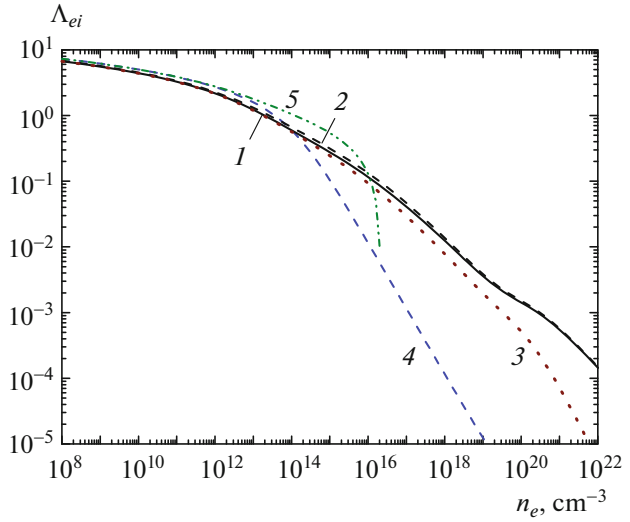

Fig. 8. (Color online) Coulomb logarithm as a function of the electron concentration at $T = 300$ K, $z_i = 1$ with the boundary value of the wavevector $q_m = q_{mZ}$ taking into account the contribution of ions to screening, $k_s = k_D$. Numeration of the curves is the same as in Fig. 3.

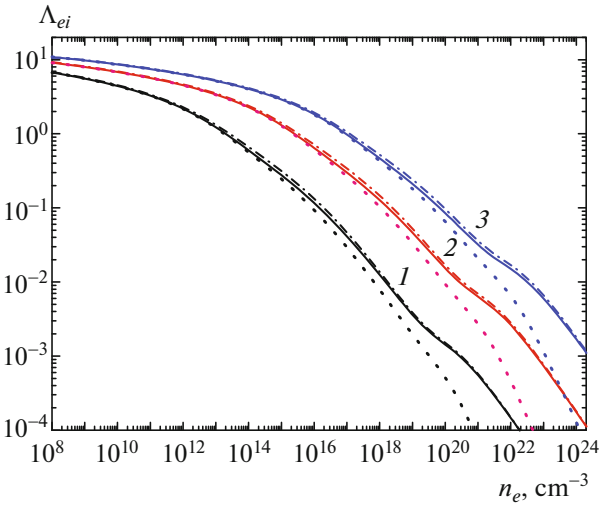

Fig. 9. (Color online) Coulomb logarithm as a function of the electron concentration for $z_i = 1$ with the boundary value of the wavevector $q_m = q_{mZ}$ taking into account the contribution of ions to screening, $k_s = k_D$ at different temperatures: 300 K (*1*); 1500 K (*2*), and 5000 K (*3*). Solid curves correspond to numerical integration of expression (17) with the static structure factor from the OZ equation in the HNC approximation; dot-and-dash curves correspond to formula (21) and dotted curves, to (23).

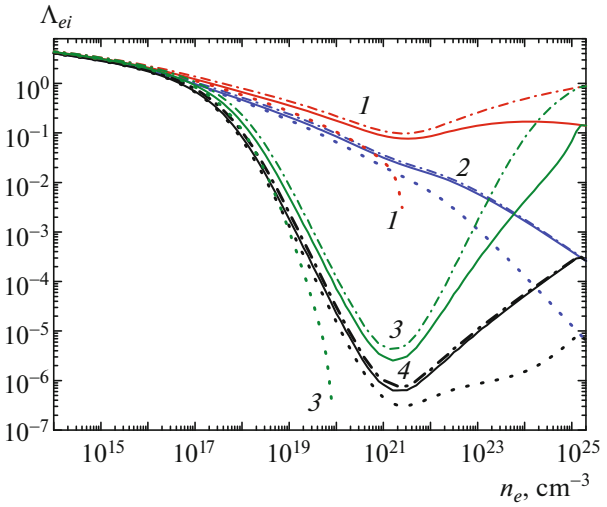

Fig. 10. (Color online) Coulomb logarithm as a function of the electron concentration for $z_i = 1$, $T = 5000$ K. Curve *1* corresponds to variant 1 with the boundary value of wavevector $q_m = q_{mZ}$ disregarding the contribution of ions to screening, $k_s = k_{De}$; (*2*) variant 2 with $q_m = q_{mZ}$ and $k_s = k_D$; (*3*) variant 3 with $q_m = q_{mS}$ and $k_s = k_{De}$; (*4*) variant 4 with $q_m = q_{mS}$ and $k_s = k_D$. Solid curves correspond to numerical integration of expression (17) with the static structure factor from the OZ equation in the HNC approximation; dot-and-dash curves correspond to formula (21) and dotted curves, to (23).

model [18, 28]:

$$\sigma_T = \frac{4e^2T^{-3/2}}{3\sqrt{\pi}m_e}\frac{2}{\lambda_e^3}\int_0^\infty \frac{\varepsilon_e^{3/2}}{\nu(\varepsilon_e)}\left(-\frac{\partial f_0}{\partial \varepsilon_e}\right)d\varepsilon_e. \qquad (31)$$

Here, ν is the transport frequency of electron collisions:

$$\nu(\varepsilon_e) = \sqrt{\frac{2\varepsilon_e}{m_e}}[n_i Q_{ei}(\varepsilon_e) + n_a Q_{ea}(\varepsilon_e)], \qquad (32)$$

where Q_{ea} and Q_{ei} are the transport cross sections of electron scattering by atoms with concentration n_a and ions with concentration n_i, respectively. If the plasma contains several species of neutral atoms (molecules) and/or ions, summation should be performed over these species of particles. In this work, we consider only the case when collisions of electrons with singly ionized ions prevail. In the general case, the collisions with neutral atoms and molecules must be taken into account, which will reduce the electrical conductivity of the plasma; for this reason, the values obtained in this study determine the upper boundary of the electrical conductivity.

In the case when the electron–ion collisions dominate, we have

$$\nu(\varepsilon_e) = \pi z_i^2 e^4 \Lambda_{ei}\sqrt{\frac{2}{m_e}}n_i\varepsilon_e^{-3/2}. \qquad (33)$$

Using relation (32), we obtain from (31)

$$\sigma_T = \frac{2T}{\pi z_i e^2 \Lambda_{ei}}\sqrt{\frac{8T}{\pi m_e}}\frac{\mathcal{F}_2(\eta_e)}{\mathcal{F}_{1/2}(\eta_e)}. \qquad (34)$$

Figure 11 shows the dependences of the electrical conductivity for the four variants of selection of the boundary value of the wavevector and the screening constant. It can be seen that the lowest values of the conductivity are obtained in the calculations with variant 1 ($k_s = k_{De}$ and $q_m = q_{mZ}$); the results obtained in variant 3 ($k_s = k_{De}$ and $q_m = q_{mS}$) begin to approach these values for high electron concentrations. It can be seen from Fig. 11 that the values of the conductivity with the unit value of the Coulomb logarithm for $n_e > 10^{17}$ cm^{-3} are lower than in all four variants.

Figure 11 also shows the values of the electrical conductivity of the plasma, which were obtained in [18] taking into account the contribution of neutral atoms and molecules to electron scattering, and the Coulomb logarithm was calculated by formula (23) as in variant 4 (see dotted curve *4* in Fig. 10). The contribution of neutral atoms and molecules to the total scattering cross section turned out to be overwhelming. Figure 11 also shows the experimental values of the plasma conductivity measured in [39–43]. For determining the electron concentration from the number density or concentration of atoms and molecules of the neutral gas, we used the results of calculations [18]; the recalculation was performed at a tem-

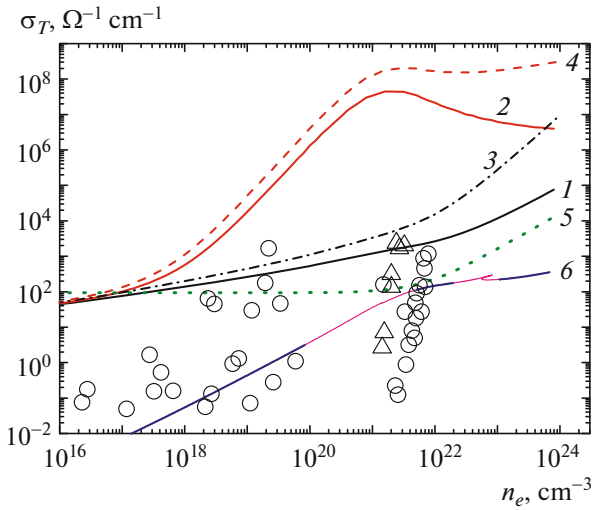

Fig. 11. (Color online) Conductivity in the case when scattering of electrons by ions prevails at $T = 5000$ K, $z_i = 1$. Curve *1* corresponds to variant 1 ($q_m = q_{mZ}$, $k_s = k_{De}$); (*2*) variant 2 ($q_m = q_{mZ}$, $k_s = k_D$); (*3*) variant 3 ($q_m = q_{mS}$, $k_s = k_{De}$); (*4*) variant 4 ($q_m = q_{mS}$, $k_s = k_D$); (*5*) calculation with $\Lambda_{ei} = 1$; (*6*) calculation [18]; (○) experimental data from [40, 41]; (△) experimental data from [42].

perature of 5000 K for the results obtained in [39, 41] and at 2500 K for the data from [42]. It can be seen that a number of experimental points are above curves *1* and *5*; for this reason, the results of calculations with the Coulomb logarithm as in variant 1 and for $\Lambda_{ei} = 1$ are in worse agreement with experimental data from [39–43] than in calculations in the three remaining variants when electron scattering by neutral hydrogen atoms and molecules is taken into account.

5. CONCLUSIONS

The investigations carried out in this study have shown that the values of the Coulomb logarithm strongly depend on the choice of the boundary value of the wavevector and on the choice of the method for determining the ion screening constant taking into account or disregarding this contribution. The effect of the ion–ion correlation in a nondegenerate plasma is found to be weak, while in the degenerate plasma, this correlation must be taken into account only in the case when the ion–ion interaction potential is determined by the screening by the electron component alone. Comparison of the calculated values of the electrical conductivity of the hydrogen plasma with the experimental values obtained in the megabar region of pressures have shown that the values of the Coulomb logarithm that are much smaller than unity can indeed exist. A more accurate determination of the Coulomb logarithm requires the planning and running of special experiments.

Small values of the Coulomb logarithm at high pressures make scattering by neutral atoms and molecules a dominating process (in hydrogen up to densities on the order of 1 g/cm^3) despite the above-mentioned ionization by pressure and the high degree of ionization of the gas. Since the frequency of electron–ion collisions is strongly reduced by the small Coulomb logarithm, electrons in a nonideal dense plasma can be "magnetized" quite easily in moderate magnetic fields of about 1 T. At extremely high pressures and gas densities (this range of densities for hydrogen is above 5 g/cm^3), scattering of electrons by ions prevails over scattering by neutral atoms and molecules. For this reason, the electron transfer coefficients in such conditions are determined by collisions of electrons with ions and not with neutral atoms. The electrical and thermal conductivities of the plasma in this case may turn out to be comparable with or higher than their values in metals. At high temperatures, the heat transfer is determined by heat conduction; therefore, the electron thermal conductivity plays an insignificant role; however, its value on a low-temperature plasma can be significant. This paves ways for experimental verification of various theories of electron transport in a nonideal plasma, including the methods for determining the Coulomb logarithm. The electrical (and thermal) conductivity in a magnetic field across this field cannot be extremely high and can be measured experimentally.

ACKNOWLEDGMENTS

This study was supported by the Russian Science Foundation (project no. 16-12-10511).

REFERENCES

1. L. D. Landau, Zh. Eksp. Teor. Fiz. **7**, 203 (1937).
2. L. Spitzer, Mon. Not. R. Astron. Soc. **100**, 396 (1940).
3. R. S. Cohen, L. Spitzer, Jr., and P. McR. Routly, Phys. Rev. **80**, 230 (1950).
4. L. Spitzer, Jr. and R. Härm, Phys. Rev. **89**, 977 (1953).
5. L. Spitzer, Jr., *Physics of Fully Ionized Gases* (Interscience, London, 1956).
6. S. V. Temko, Sov. Phys. JETP **4**, 898 (1956).
7. O. V. Konstantinov and V. I. Perel', Sov. Phys. JETP **14**, 944 (1961).
8. S. Skupsky, Phys. Rev. A **16**, 727 (1977).
9. Y. T. Lee and R. M. More, Phys. Fluids **27**, 1273 (1984).
10. C.-K. Li and R. D. Petrasso, Phys. Rev. Lett. **70**, 3063 (1993).
11. C. A. Ordonez and M. I. Molina, Phys. Plasmas **1**, 2515 (1994).
12. E. Bésuelle, R. R. E. Salomaa, and D. Teychenné, Phys. Rev. E **60**, 2260 (1999).
13. T. S. Ramazanov and S. K. Kodanova, Phys. Plasmas **8**, 5049 (2001).
14. J. R. Correa, Y. Chang, and C. A. Ordonez, Phys. Plasmas **12**, 084505 (2005).

15. D. O. Gericke, M. S. Murillo, and M. Schlanges, Phys. Rev. E **65**, 036418 (2002).
16. L. S. Brown and R. L. Singleton, Jr., Phys. Rev. E **76**, 066404 (2007).
17. L. G. Stanton and M. S. Murillo, Phys. Rev. E **93**, 043203 (2016).
18. A. N. Starostin, V. K. Gryaznov, and A. V. Filippov, JETP Lett. **104**, 696 (2016).
19. V. E. Fortov, Phys. Usp. **50**, 333 (2007).
20. J. M. Ziman, Philos. Mag. **6**, 1013 (1961).
21. J. M. Ziman, Proc. Phys. Soc. **86**, 337 (1965).
22. J. M. Ziman, Adv. Phys. **13**, 89 (1964).
23. C. C. Bradley, T. E. Faber, E. G. Wilson, and J. M. Ziman, Philos. Mag. **7**, 865 (1962).
24. J. M. Ziman, Adv. Phys. **16**, 551 (1967).
25. E. M. Livshits and L. P. Pitaevskii, *Course of Theoretical Physics*, Vol. 10: *Physical Kinetics* (Nauka, Moscow, 1979; Pergamon, Oxford, 1981).
26. R. B. Dingle, Philos. Mag. J. Sci. **46**, 831 (1955).
27. M. Goano, ACM Trans. Math. Software **21**, 221 (1995).
28. V. K. Gryaznov, Yu. V. Ivanov, A. N. Starostin, and V. E. Fortov, Teplofiz. Vys. Temp. **14**, 643 (1976).
29. R. Barrie, Proc. Phys. Soc. B **69**, 553 (1956).
30. L. D. Landau and E. M. Lifshitz, Course of Theoretical Physics, Vol. 5: Statistical Physics (Fizmatlit, Moscow, 2002; Pergamon, Oxford, 1980).
31. I. Z. Fisher, Sov. Phys. Usp. **5**, 239 (1962).
32. N. P. Kovalenko and I. Z. Fisher, Sov. Phys. Usp. **15**, 592 (1972).
33. G. N. Sarkisov, Phys. Usp. **42**, 545 (1999).
34. T. Morita and K. Hiroike, Progr. Theor. Phys. **23**, 1003 (1960).
35. Yu. V. Arkhipov, A. Askaruly, A. E. Davletov, D. Yu. Dubovtsev, Z. Donkó, P. Hartmann, I. Korolov, L. Conde, and I. M. Tkachenko, Phys. Rev. Lett. **119**, 045001 (2017).
36. A. V. Filippov, A. N. Starostin, I. M. Tkachenko, and V. E. Fortov, Phys. Lett. A **376**, 31 (2011).
37. A. V. Filippov, A. N. Starostin, I. M. Tkachenko, and V. E. Fortov, Contrib. Plasma Phys. **53**, 442 (2013).
38. K.-C. Ng, J. Chem. Phys. **61**, 2680 (1974).
39. S. T. Weir, A. C. Mitchell, and W. J. Nellis, Phys. Rev. Lett. **76**, 1860 (1996).
40. V. E. Fortov, V. Ya. Ternovoi, S. V. Kvitov, V. B. Mintsev, D. N. Nikolaev, A. A. Pyalling, and A. S. Filimonov, JETP Lett. **69**, 926 (1999).
41. V. Ya. Ternovoi, A. S. Filimonov, V. E. Fortov, S. V. Kvitov, D. N. Nikolaev, and A. A. Pyalling, Phys. B: Condens. Matter **265**, 6 (1999).
42. W. J. Nellis, S. T. Weir, and A. C. Mitchell, Phys. Rev. B **59**, 3334 (1999).
43. R. Chau, A. C. Mitchell, R. W. Minich, and W. J. Nellis, Phys. Rev. Lett. **90**, 245501 (2003).

Translated by N. Wadhwa